Experimentální Analýza Napětí 2007

NUMERICAL STUDY ON A CROSS-SHAPED SPECIMEN UNDER BIAXIAL TENSION

Ladislav Écsi,[1] Pavel Élesztős[2]

Abstract: The aim of the paper is to investigate the thermo-mechanical behavior of a cross-shaped specimen under biaxial tension. In the numerical study a new energy conservation equation for fully coupled thermal structural finite element analysis was used utilizing the updated Lagrange method for large strain/large deflection formulation and the NoIHKH material model for cyclic plasticity of metals using associative plasticity with combined kinematic and isotropic hardening. The calculation results were compared with the available experimental results.

Keywords: *new energy conservation equation, fully coupled thermal-structural analysis, finite element method, cyclic plasticity of metals*

1. Introduction

The phenomenon that a solid body changes its temperature under mechanical loading has been known for long time. The thermodynamics of the process however has never been properly understood. Up to now several heat equations have been proposed to model solid body thermo-mechanical behaviour [1], although none of their results can be considered satisfactory. Moreover, most of them are based on the internal energy material derivative formulation, which was derived as a result of a mathematically manipulated energy conservation equation with unknown internal energy term. In this paper the authors present a new energy conservation equation [3], which formally takes into account all mechanical and thermal energy contributions. Under the word "formally" we mean that the equation is complete with respect to the number of its terms, however some of the terms might still be considered vague, which enables further improvement, such as considering the plastic heating via a heat generation rate per unit volume. Although, the equation various application has already been shown [4], [5], more experiments are needed to investigate how much its results correspond with reality.

In this paper a numerical study on a cross-shaped specimen under biaxial tension is presented using the new equation. The calculation results will be compared with the available experimental results.

2. Theory background

In the numerical study the finite element method (FEM) was used utilizing a fully coupled thermal structural analysis and large strain / large deflection formulation with the updated Lagrange method. The governing equations to describe deformable body behaviour are the force equilibrium equation and the energy conservation equation expressed in the following variational forms:

[1] Ing. Ladislav Écsi, SjF. STU Bratislava SR, Námestie slobody 17, 812 31 Bratislava 1, tel.: +421 2 5292 6620, e-mail: ladislav.ecsi@stuba.sk

[2] Doc. Ing. Pavel Élsztős CSc., SjF. STU Bratislava SR, Námestie slobody 17, 812 31 Bratislava 1, tel.: +421 2 5292 6620, e-mail: pavel.elesztos@stuba.sk

$$\int_{\Omega}\rho\dot{\mathbf{v}}\bullet\delta\mathbf{v}dv+\int_{\Omega}\boldsymbol{\sigma}:\delta\mathbf{d}dv=\int_{\Omega}\mathbf{b}\bullet\delta\mathbf{v}dv+\int_{\partial\Omega}\mathbf{t}\bullet\delta\mathbf{v}ds+\sum_{i=1}^{NNode}\mathbf{f}_i\bullet\delta\mathbf{v}_i\,, \tag{1}$$

$$\begin{aligned}&\int_{\Omega}\delta T\rho\dot{\mathbf{v}}\bullet\mathbf{v}dv+\int_{\Omega}\delta T(\boldsymbol{\sigma}:\mathbf{d})dv+\int_{\Omega}(\nabla\delta T)\bullet(\boldsymbol{\sigma}\bullet\mathbf{v})dv+\int_{\Omega}\delta T\rho c\dot{T}dv-\int_{\Omega}(\nabla\delta T)\bullet\mathbf{q}dv=\\&=\int_{\Omega}\delta T\mathbf{b}\bullet\mathbf{v}dv+\int_{\partial\Omega}\delta T\mathbf{t}\bullet\mathbf{v}ds+\int_{\partial\Omega}\delta Tq_n ds+\int_{\Omega}\delta Trdv+\sum_{i=1}^{NNode}\delta T_i\mathbf{f}_i\bullet\mathbf{v}_i+\sum_{i=1}^{NNode}\delta T_iQ_i\end{aligned} \tag{2}$$

with

$$\mathbf{q}=-\mathbf{K}\bullet(\nabla T)\,.$$

In equations (1), (2) $\mathbf{v},T$ are the velocity vector and the temperature $\boldsymbol{\sigma},\mathbf{d},\mathbf{K}$ stand for the Cauchy stress tensor, the strain rate tensor and the heat conductivity tensor $\mathbf{b},\mathbf{t},\mathbf{f}_i,\mathbf{q},q_n,r,Q_i$ denote the volume force vector, surface traction vector, nodal force vector, heat flux vector, normal heat flux, heat generation rate per unit volume and nodal heat flux and ρ,c represent the material density and specific heat respectively.

Considering that the strain rate tensor has the additive decomposition $\mathbf{d}=\mathbf{d}^e+\mathbf{d}^p+\alpha\dot{T}\mathbf{I}$, where $\mathbf{d}^e,\mathbf{d}^p$ stand for its elastic and plastic parts, α is the coefficient of thermal expansion and $\mathbf{I}$ is an identity tensor, eqs. (1) and (2) are supplemented with the following constitutive and evolution equations:

$$f=\sigma_{eq}-\sigma_y-R\le 0\,,\sigma_{eq}=\sqrt{\frac{3}{2}\left(\hat{\boldsymbol{\Sigma}}-\hat{\mathbf{X}}\right):\left(\hat{\boldsymbol{\Sigma}}-\hat{\mathbf{X}}\right)}\,,R=Q\left(1-e^{\left(-b\varepsilon^p\right)}\right), \tag{3}$$

$$\hat{\dot{\mathbf{X}}}=\mathbb{C}_{cycl}:\hat{\mathbf{d}}^p-\gamma\left(\varepsilon^p\right)\hat{\mathbf{X}}\dot{\varepsilon}^p\,,tr\left(\hat{\mathbf{X}}\right)=0\,,\ \gamma\left(\varepsilon^p\right)=\gamma_\infty-\left(\gamma_\infty-\gamma_0\right)e^{\left(-\omega\varepsilon^p\right)}, \tag{4}$$

$$\mathbb{C}_{cycl}=2G_{cycl}\mathbb{I}+\lambda_{cycl}\left(\mathbf{I}\otimes\mathbf{I}\right),G_{cycl}=\frac{E_{cycl}}{2\left(1+\mu_{cycl}\right)},\lambda_{cycl}=\frac{\mu_{cycl}E_{cycl}}{\left(1+\mu_{cycl}\right)\left(1-2\mu_{cycl}\right)}. \tag{5}$$

Equations (3)-(5) represent the extended NoIHKH material model for cyclic plasticity of metals [2], modified for large strain/ large deformation, using combined isotropic and kinematic hardening with associative plasticity, where $\mathbb{C}_{cycl}$ is a fourth order cyclic material tensor $\mathbb{I},\hat{\boldsymbol{\Sigma}},\hat{\mathbf{X}},\hat{\mathbf{d}}^P$ are the 4th order unit tensor, the corotational deviatoric stress tensor, the corotational back stress tensor and the corotational plastic strain rate tensor, $\varepsilon^p,\dot{\varepsilon}^p$ denote the accumulated plastic strain and the accumulated plastic strain rate and $Q,b,\gamma_0,\gamma_\infty,\omega,\mu_{cycl},E_{cycl}$ stand for the material properties. In the Cauchy stress update calculation and also in the corotational back stress evolution equation (4) derivation there was used the Jaumann objective rate in the form of the Green-Naghdi objective rate utilizing the following rotation tensors at the midpoint and endpoint configuration of the body:

$$\mathbf{R}^{n+\frac{1}{2}}=\exp\left[\frac{\Delta t}{2}\mathbf{W}^{n+\frac{1}{2}}\right]\bullet\mathbf{R}^n\,, \tag{6}$$

$$\mathbf{R}^{n+1}=\exp\left[\Delta t\mathbf{W}^{n+\frac{1}{2}}\right]\bullet\mathbf{R}^n\,. \tag{7}$$

where $\mathbf{W}^{n+\frac{1}{2}}$ is the spin tensor at midpoint configuration, $\mathbf{R}^n$ stands for the rotation tensor at the previous configuration and Δt denotes the time step value. The tensor exponential function was expressed with the Rodriguez formula. The plastic heating of the body was achieved via a heat generation rate per unit volume, expressed as 80% of the internal plastic power, which means that 80% of the dissipated plastic work has changed into heat:

$$r = 0.8\boldsymbol{\sigma} : \mathbf{d}^p . \tag{8}$$

2.1 Time discretization issues

In this calculation the simplest time discretization scheme was used. Let variable x denote either the nodal temperature or the nodal deformation vector in the calculation.

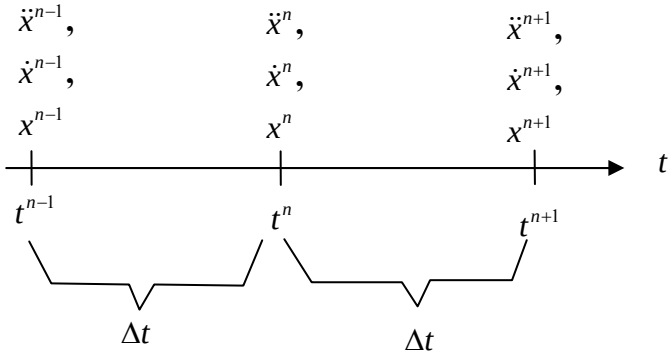

Fig. 1. Time discretisation

Considering figure 1 and constant time step, the average velocity of the variable x in the time interval $\left(t^n, t^{n+1}\right\rangle$ and $\left(t^{n-1}, t^n\right\rangle$ can be calculated as follows

$$\dot{x}^{n,n+1}_{average} = \frac{x^{n+1} - x^n}{\Delta t}, \qquad \dot{x}^{n-1,n}_{average} = \frac{x^n - x^{n-1}}{\Delta t}. \tag{9}$$

Similarly, the average acceleration of the variable x in the time interval $\left(t^n, t^{n+1}\right\rangle$ can be calculated according to the following formula:

$$\ddot{x}^{n,n+1}_{average} = \frac{\dot{x}^{n+1} - \dot{x}^n}{\Delta t}. \tag{10}$$

If we don't know, how the velocity and acceleration changes with time, we can simply use the definitions (9) and (10) at the end points of the time intervals:

$$\dot{x}^{n+1} \approx \dot{x}^{n,n+1}_{average}, \qquad \dot{x}^{n} \approx \dot{x}^{n-1,n}_{average}, \qquad \ddot{x}^{n+1} \approx \ddot{x}^{n,n+1}_{average}, \tag{11}$$

from which the following formulas can be derived for the x variable velocity and acceleration at time t^{n+1}:

$$\dot{x}^{n+1} = \frac{x^{n+1} - x^n}{\Delta t}, \qquad \ddot{x}^{n+1} = \frac{x^{n+1} - 2x^n + x^{n-1}}{\Delta t^2}. \tag{12}$$

In commercial codes it is usually presumed, that the velocity and acceleration of the variable x changes linearly between the discrete times t^{n-1}, t^n, t^{n+1}. Then applying the trapezoidal rule we can rewrite the corresponding average values as follows:

$$\dot{x}^{n,n+1}_{average} \cong \frac{\dot{x}^{n+1}+\dot{x}^{n}}{2}, \qquad \dot{x}^{n-1,n}_{average} \cong \frac{\dot{x}^{n}+\dot{x}^{n-1}}{2}, \qquad \ddot{x}^{n,n+1}_{average} = \frac{\ddot{x}^{n+1}+\ddot{x}^{n}}{2}, \tag{13}$$

which after being supplemented with equations (9) and (10) will imply the following formulas for the x variable velocity and acceleration at time t^{n+1}:

$$\dot{x}^{n+1} = \frac{2}{\Delta t}\left(x^{n+1}-x^{n}\right)-\dot{x}^{n}, \qquad \ddot{x}^{n+1} = \frac{4}{\Delta t^{2}}\left(x^{n+1}-x^{n}\right)-\frac{4}{\Delta t}\dot{x}^{n}-\ddot{x}^{n}. \tag{14}$$

Both time discretisation schemes (12), (14) are acceptable from the mathematical point of view, however their results might slightly differ.

3. Numerical example

As a numerical example a cross shaped specimen under biaxial tension was studied. Figure 2 depicts the specimen geometry, the body of which contains 60mm long and 0.2mm wide axial cuts, to homogenize the stress field at its centre. In the numerical study only 1/8 of the specimen was modelled (Fig. 3) employing 3 planes of symmetry. As a simplification, no fillets and no axial cuts were modelled. The body was loaded gradually using 0.5mm maximum prescribed axial deformation at its four ends. The deformation was applied as a ramped load and the maximum prescribed displacement was achieved in 10 substeps. In the analysis an 8 node three-dimensional solid element with linear shape functions was used. Heat convection through all surfaces was considered, applying zero bulk/environmental temperature. The body was initially at rest with zero initial temperature. Analyses with and without heat generation rate per unit volume were carried out. The calculations were run as transient-dynamic ones, using a time step of 1.0 second.

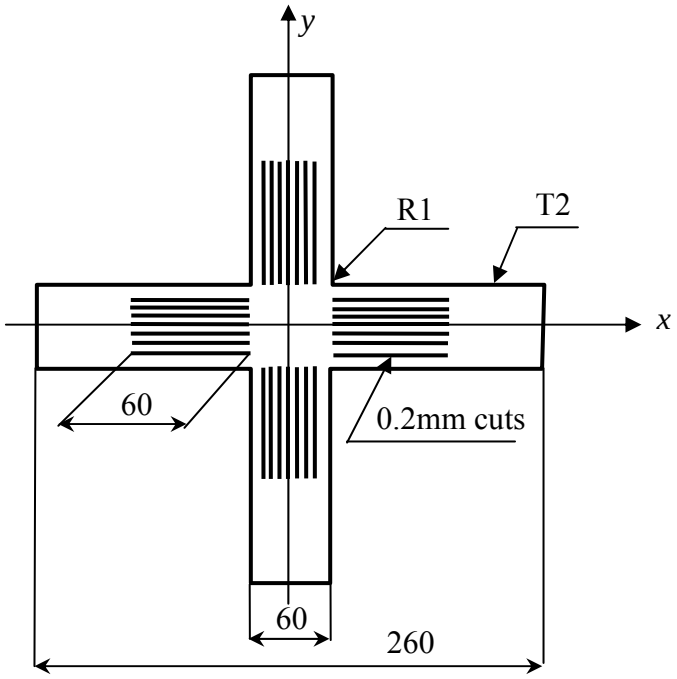

Fig. 2. Specimen geometry

In the numerical study low carbon steel material properties were used, which were considered to be constant. The used cyclic material properties however are not necessarily

correct since we couldn't make experimental tests. Table 1 outlines the employed material properties.

$c = 450.0\,\mathrm{J}\Big/\left(\mathrm{kg}\cdot\mathrm{C}^{\circ}\right)$	$\mu = 0.29$
$k = k_{xx} = k_{yy} = k_{zz} = 80.4\ W/\left(m\cdot C^{\circ}\right)$	$\mu_{cycl} = 0.25$
$\alpha = \alpha_x = \alpha_y = \alpha_z = 0.0000123\ C^{\circ -1}$	$\sigma_y = 275000000.0\ Pa$
$h = 50.0\ W/\left(m^2\cdot C^{\circ}\right)$	$Q = 275000000.0\ Pa$
$T_{bulk} = 0.0C^{\circ}$	$b = 3.0$
$\rho = 7800.0kg/m^3$	$\gamma_{\infty} = 20.0$
$E = 211000000000.0\ Pa$	$\gamma_0 = 10.0$
$E_{cycl} = 211000000000.0\ Pa$	$\omega = 10.0$

Tab. 1. Material properties

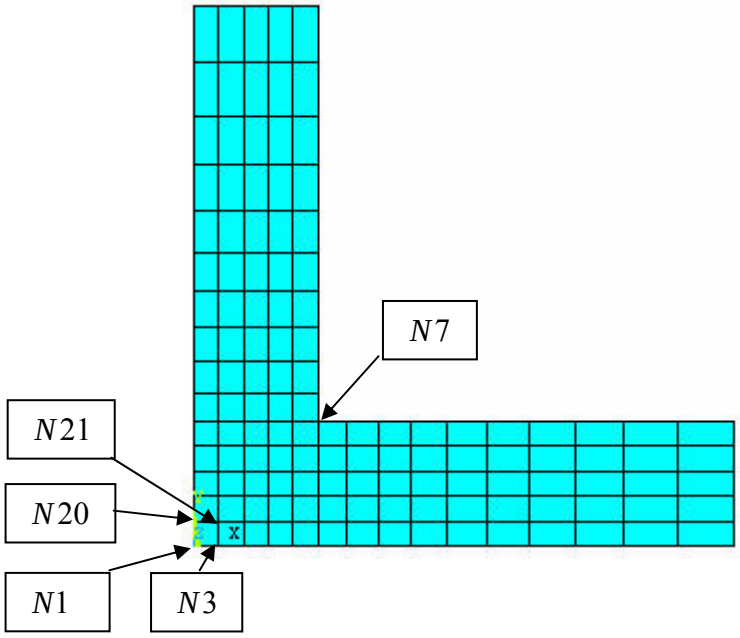

Fig. 3. Finite element mesh

4. Numerical results

In figures 4-7 can be seen the displacement vector sum, the temperature field, the Von Mises stress distribution and the accumulated plastic strain distribution at the end (at time 10 seconds) of the analysis without considering the plastic heating (8). Figure 8 shows in colour how the negative temperature regions evolve as a function of time. As can be seen, there are certain areas, where the temperature is bellow zero permanently. To make further investigation time history curves were created at selected nodes. The nodes are located at the centre of the specimen and they are denoted as N1, N3, N21 and N20 in figure 3. Figure 9 shows the corresponding temperature time history curves. As we can see, the curves, coming from the analysis where no plastic heating was considered, are complete, however the calculation which takes into account the effect of the plastic heating, is still running and that is why the corresponding curves are still incomplete.

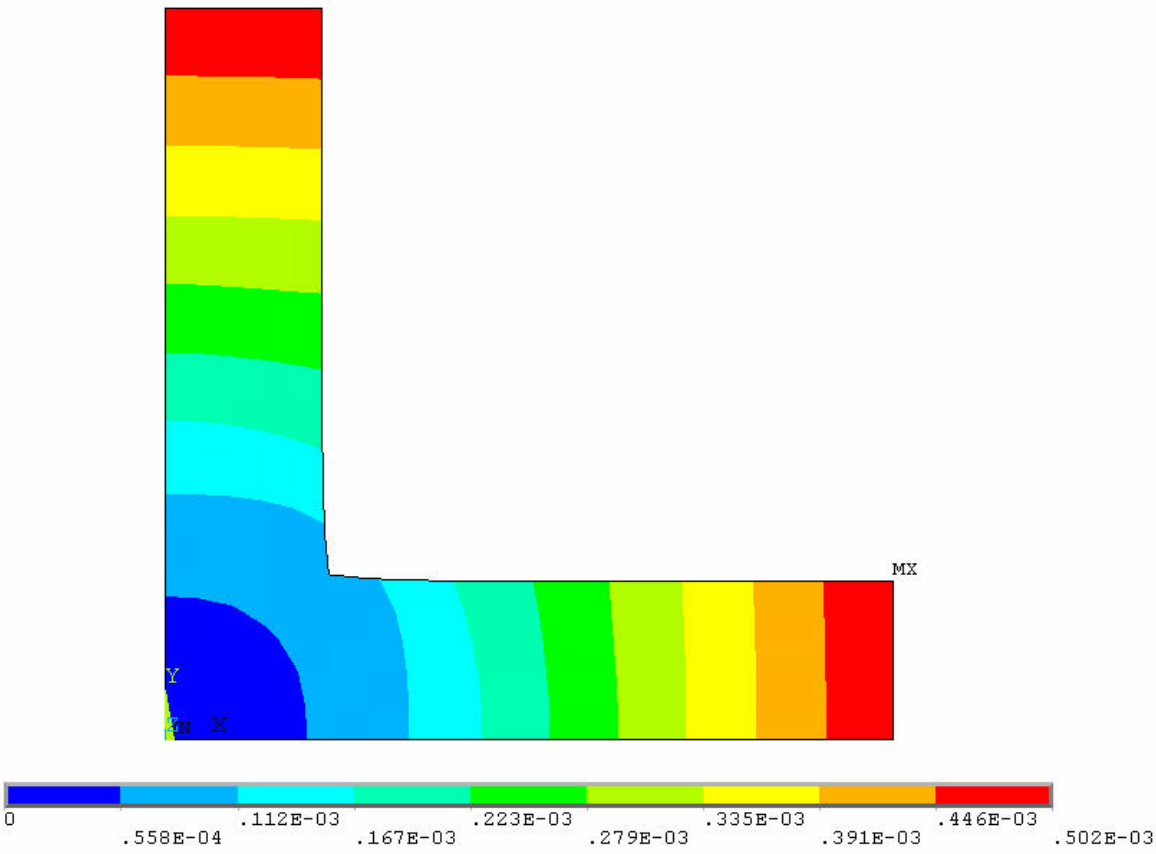

Fig. 4. Displacement vector sum at the end of the analysis in meters

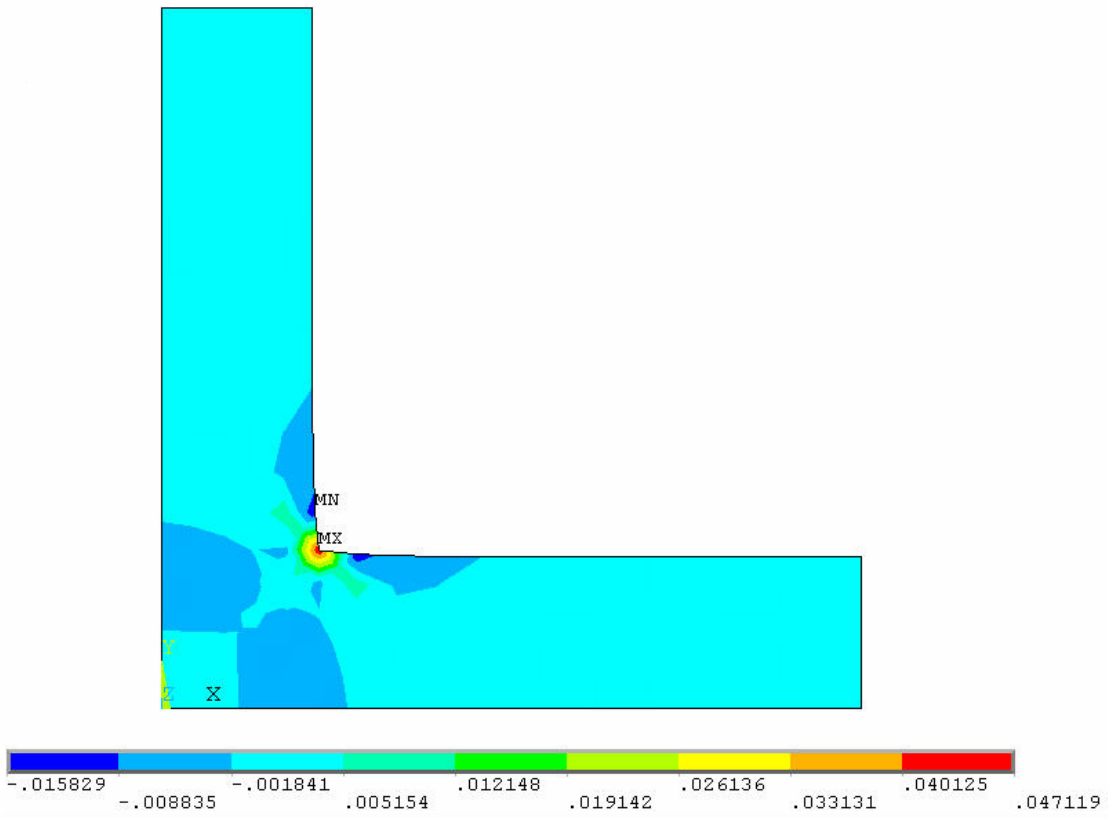

Fig. 5. Temperature field at the end of the analysis in centigrades

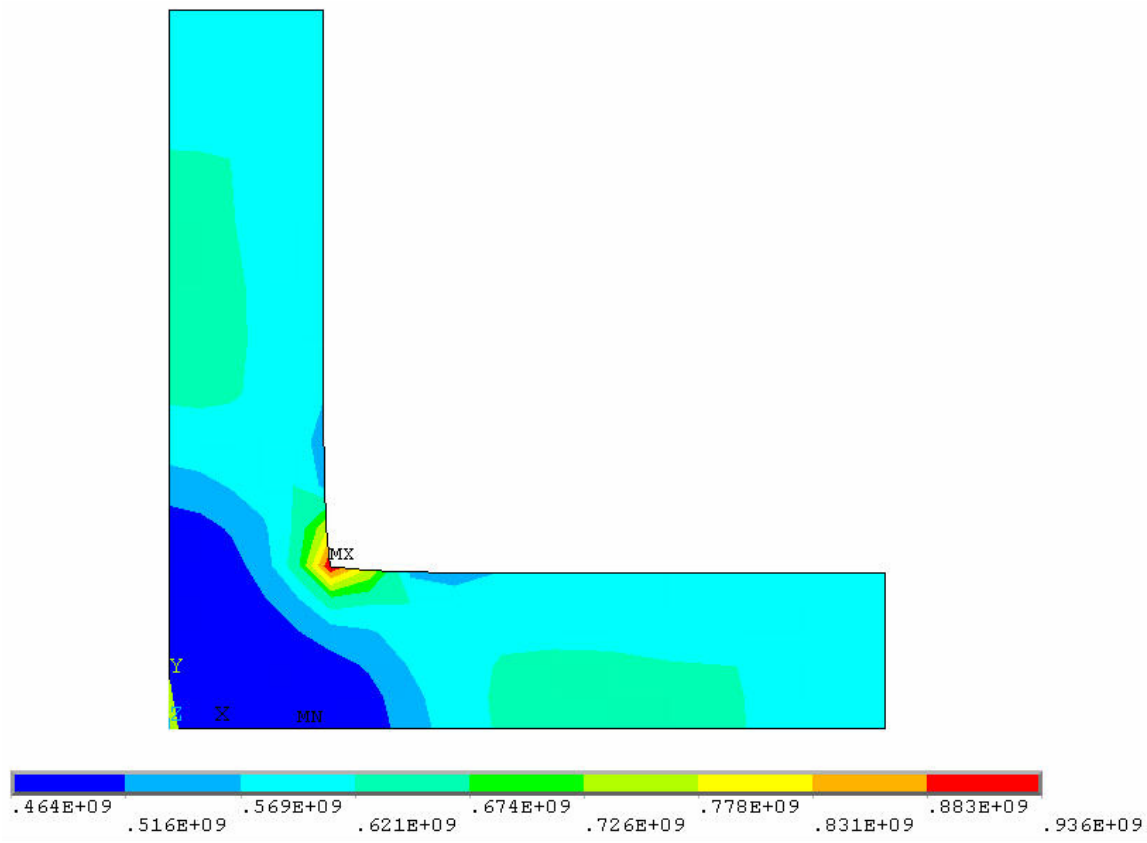

Fig. 6. Von Mises stress at the end of the analysis in pascals

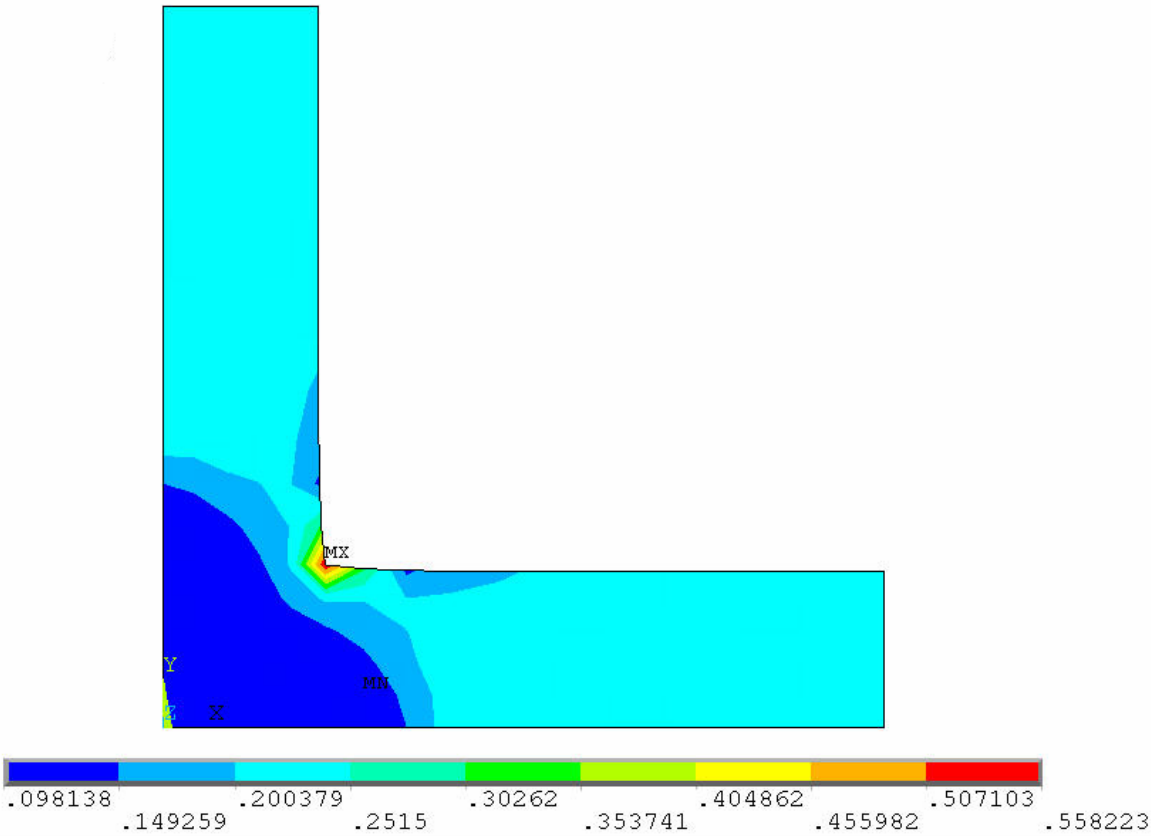

Fig. 7. Accumulated plastic strain

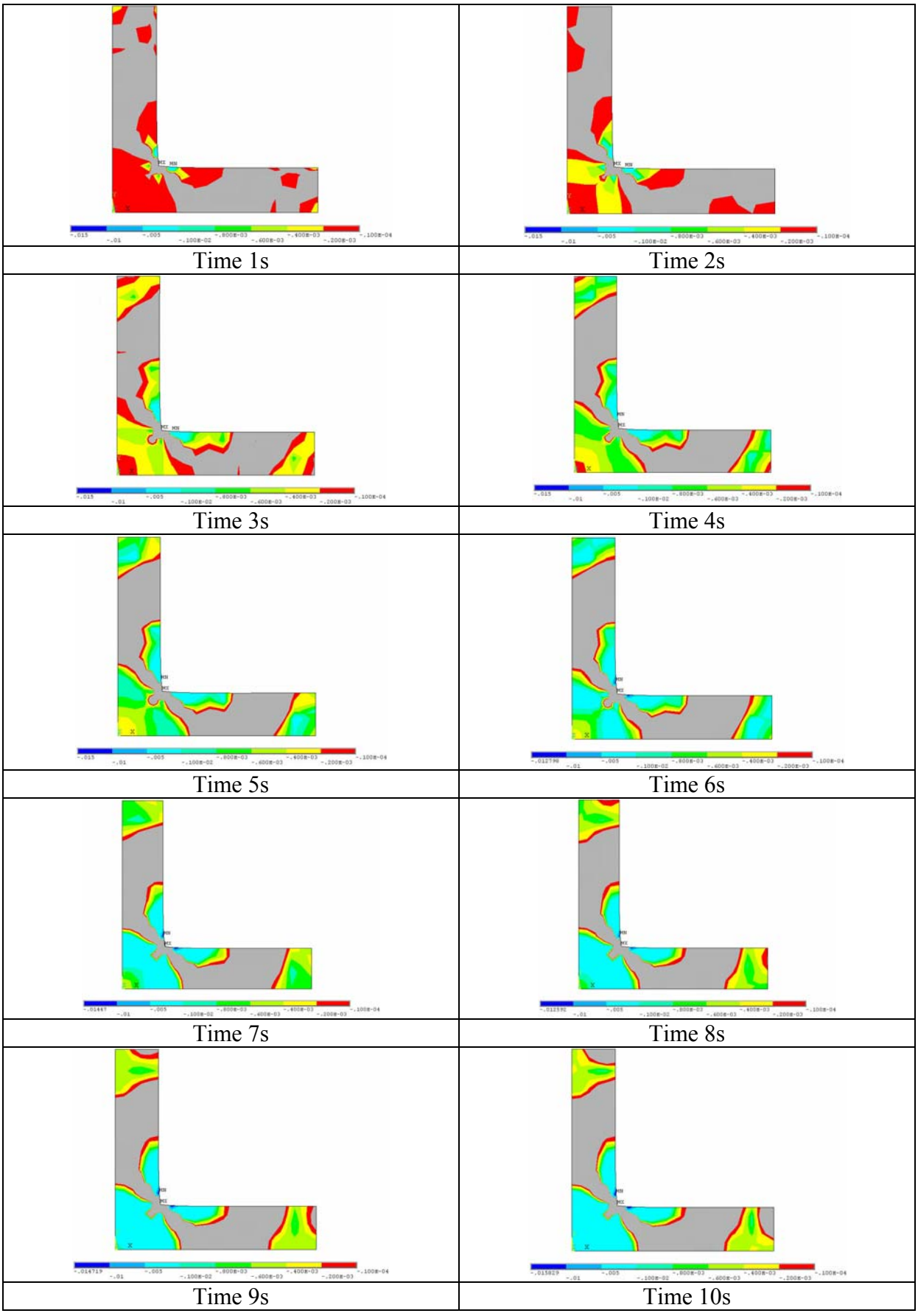

Fig. 8. Negative temperature regions are depicted in colour

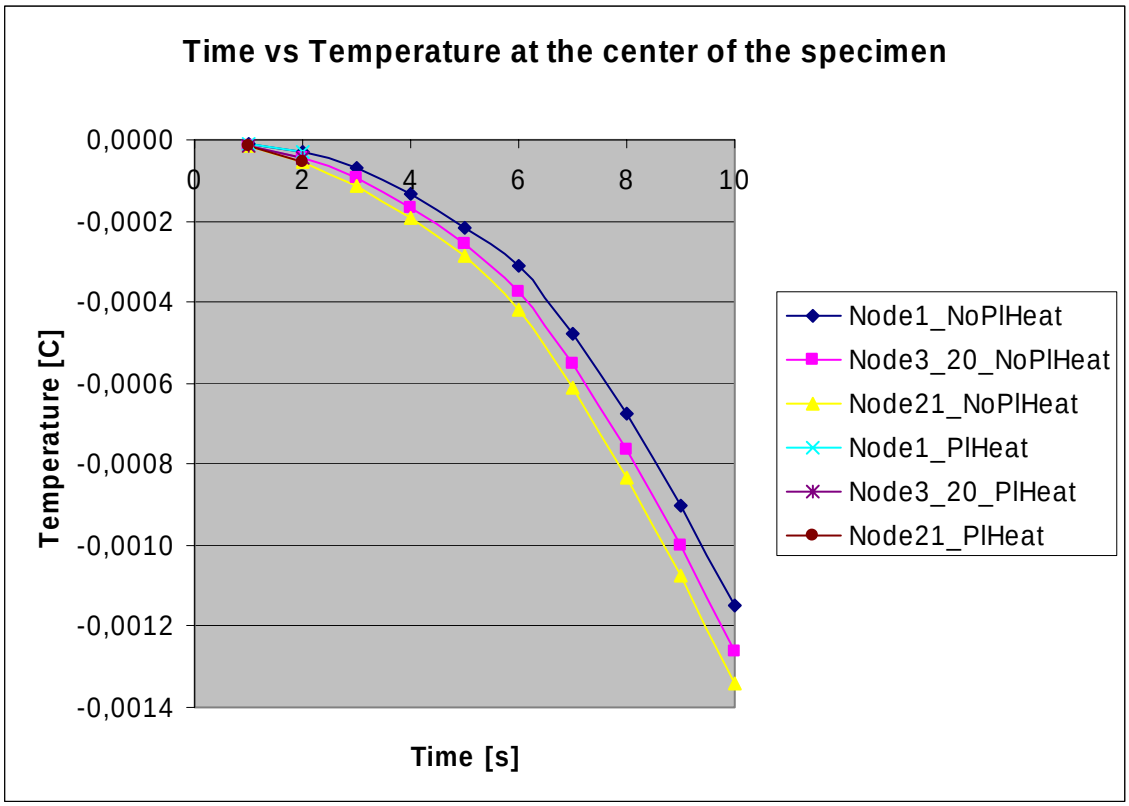

Fig. 9. Temperature time history curves at selected nodes

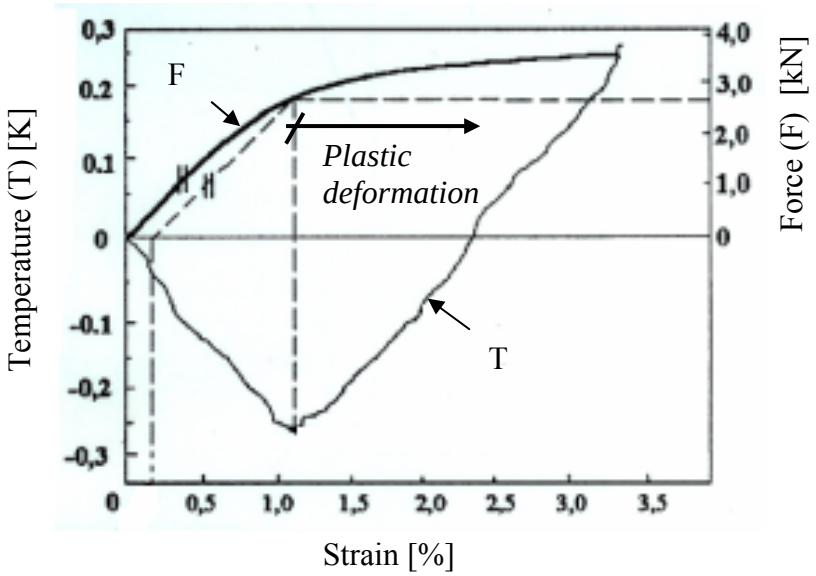

Fig. 10. Biaxial test on an AlMgSi1 specimen after Franke H [6],[7]

Figure 10 shows the biaxial test result on an AlMgSi1 specimen after Franke H [6], found in [7]. In the test the temperature measurement was carried out at the centre of the specimen. As we can see in figure 10, the temperature decreases in the elastic region until the material yield stress is reached. When plastic deformation takes place, the temperature reaches its minimum then it increases as the deformation continues. Although the numerical calculation results differ in orders of magnitude from the experimental results, the phenomenon of the temperature decrease at the centre of the specimen can be observed in both cases.

At this point it is necessary to emphasise that in the two tests different material was used. In our numerical study a low carbon steel material properties were employed, while in the experiment an aluminium specimen was used. In fact, many details of the experimental test are still unknown, such us the loading rates, the used material properties, the specimen geometry and the temperature sensor exact location, which make the comparison extremely difficult.

5. Conclusion

In this paper a numerical study on a cross shaped specimen under biaxial tension was carried out using fully coupled thermal structural analysis with new energy conservation equation. The analysis utilizes large strain/ large deflection formulation and the extended NoIHKH material model for cyclic plasticity of metals. In the numerical study temperature decrease was observed at the centre of the cross shaped specimen. The same phenomenon was reported in the only experimental test on a cross shaped specimen, which the authors consider to be positive. In spite of the capability of the new energy conservation equation to reproduce the phenomenon of the cooling at the centre of the specimen, at this time it is too early to draw any conclusion about the calculation results. More detailed experimental and numerical tests are needed to verify the equation properly.

Acknowledgements: Funding using the VEGA grant No 1/20084/05 resources is greatly appreciated.

References

[1] Batra, R.C., Love, B.M.: *Mesoscale analysis of shear bands in high strain rate deformations of tungsten/ nickel-iron composites*, Journal of Thermal Stresses, 2005, 28 (6-7): 747-782.

[2] Écsi, L.: *Extended NoIHKH model usage for cyclic plasticity of metals*, Engineering Mechanics, 2006, 13 (2): 83-92.

[3] Écsi, L.: *Numerical behavior of a solid body under various mechanical loads using finite element method with new energy balance equation for fully coupled thermal-structural analysis*, In proceedings of the 6th International Congress on Thermal Stresses, TS2005, Vienna, Austria, 26-29. May 2005, 543-546.

[4] Écsi, L., Élesztős, P.: *An attempt to simulate more precisely the behavior of a solid body using new energy conservation equation for fully coupled thermal-structural analysis*, In proceedings of the 3rd European Conference on Computational Mechanics, ECCM2006, Lisbon, Portugal, 5-8. June 2006.

[5] Écsi, L.: *A new energy conservation equation application in fully coupled thermal structural analysis with phase changes using finite element method (FEM)*, In proceedings of the 10th World Multi-Conference on Systemics, Cybernetics and Informatics, WMSCI2006, Orlando, Florida, USA, 16-19. July 2006.

[6] Franke, H.: *Lexikon der Physik*, Franckh'sche Verlagshandlung, W. Keller & Co, Stuttgart, 1959.

[7] Hanušovský, J.: *Kvantifikácia vzniku plastickej deformácie plechov metódami experimentálnej mechaniky*, Dizertačná práca, Katedra AM, SjF TU Košice, 2006.